15th Triennial World Congress, Barcelona, Spain

PLANNING TRAJECTORY WITH SPEED CONTROLLED MANOEUVRES FOR A TWO-LINK RIGID MANIPULATOR

Reza Fotouhi [1] **Walerian Szyszkowski** [2]
Peter N. Nikiforuk [3]

University of Saskatchewan, Saskatoon, Saskatchewan S7N 5A9, Canada

Abstract: A two part trajectory and speed planning procedure for a two-link rigid manipulator is presented. The planning is done at the joint level using cubic spline functions, and the trajectory of the robot is specified by a sequence of knots in space Cartesian coordinates. These knots are transformed into two sets of joint coordinates, and piecewise cubic spline functions are used to fit these two sets employing a time scale to construct an initial trajectory for the manipulator. Linear scaling of the time variable is used to accommodate the angular velocity and acceleration constraints imposed at the joint level. A new nonlinear time scaling scheme is then used for speed control so as to fit the manipulator's tip velocity to a pre-specified profile. Simulation results for the manipulator with payload masses following a planned trajectory are presented.

Keywords: Trajectory planning, speed control, manipulators

1. INTRODUCTION

The problem of concern in this paper is typical of many industrial manipulators. It is that of a two-link rigid manipulator required to perform a manoeuvre in which the tip is to follow a trajectory consisting of several linear segments with a predefined velocity profile. At each corner connecting two neighboring segments the tip velocity is reduced to zero so as to allow the drop off or pick up of some known tip masses. Between the corners the tip is to move either with a constant acceleration, or deceleration, or with a constant velocity. Some constraints imposed on the angular velocities and accelerations of the links must be met as well.

This task is divided into two parts: trajectory planning and speed control. The desired trajectory is given as a sequence of knots (positions of the robot's tip) between two or more corners in space Cartesian coordinates. The space coordinates of the knots are then transformed into two sets of joint coordinates. The control is performed at the joint level and it is desirable, therefore, to construct the trajectory at that level. Cubic approximation polynomials are then used to fit the sequences of knots in the joint coordinates. The functions of approximation for the trajectory in the joint coordinates pass through the given knots and are sufficiently smooth to provide for continuous motion (Schumaker, 1981; Craig, 1986).

Path planning has been studied by a number of authors. An optimum path planning problem at the joint level using cubic spline polynomials was studied by (Xiangrong and Xiangfeng, 1994). Cubic B-spline functions were used by (Thompson and Patel, 1987), and (Wang and Horng, 1990). It was claimed that, with the B-spline approach, local modification of the path was possible for one or

[1] Research Associate, Mechanical Engineering Dept., also affiliated with Red Deer College, Red Deer, Alberta, Canada
[2] Professor, Mechanical Engineering Department
[3] Dean Emeritus, College of Engineering

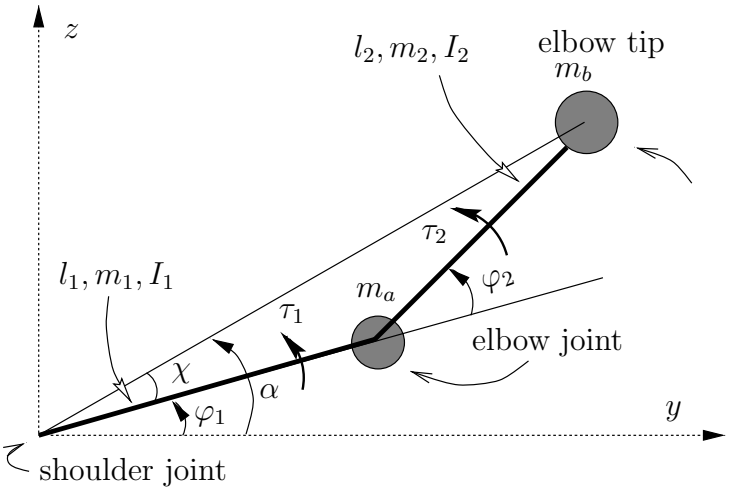

Fig. 1. Physical parameters used in formulation of two-link rigid manipulators, $l_1 = 2l_{c1} = 1.6$ $[m]$, $l_2 = 2l_{c2} = 1.6$ $[m]$, $m_1 = 1$ $[kg]$, $m_2 = 1$ $[kg]$, $m_a = 1$ $[kg]$, $m_b = 4$ $[kg]$ for $t_1 \leq t \leq t_{61}$ and $m_b = 0$ for $t_{61} < t \leq t_{121}$, $g = 0$, and $I_1 = m_1 l_1^2/12 = 0.213$ $[kg.m^2] = I_2$.

more joints without affecting the other joints. A cubic spline function was used to plan the geometric trajectory as well as for maintaining a constant speed along the geometric path by (Wu and Jou, 1991). The problem was transformed into an initial boundary value problem. Two algorithms for fine-tuning B-spline motions to obtain a near constant kinetic energy were presented by (Srinivasan and Ge, 1998). The concept of trigonometric splines was proposed by (Simon and Isik, 1991).

More specifically, in this paper the path planning is done at the joint level using cubic spline functions. To accommodate the angular velocity and acceleration constraints a linear scaling of the time variable is applied. For speed control the approach proposed by (Fotouhi *et al.*, 2000*a*) is used. This approach utilizes a nonlinear scaling of the time variable to fit the manipulator's tip velocity to a pre-specified profile. Unlike that used by (Wu and Jou, 1991), this approach can be implemented for any speed profile, not only for constant speed.

2. MANIPULATOR DYNAMICS

The equation of motion of the Two-Link Rigid Manipulator(TLRM) shown in Figure 1 in the joint space can be derived in the form

$$M(\varphi)\ddot{\varphi}(t) + Q(\varphi, \dot{\varphi}) = \tau(t) \tag{1}$$

where the mass matrix M and the force vector Q are nonlinear functions of the joint variables

$$M(\varphi) = \begin{bmatrix} a_{11} & a_{12} \\ a_{12} & a_{22} \end{bmatrix} \tag{2}$$

$$Q(\varphi, \dot{\varphi}) = \left\{ \begin{array}{c} -a_{13}(2\dot{\varphi}_1 + \dot{\varphi}_2)\dot{\varphi}_2 + a_{14}g \\ +a_{13}{\dot{\varphi}_1}^2 + a_{24}g \end{array} \right\} \tag{3}$$

and a_{ij} are known functions of the physical parameters and rotations (φ_1, φ_2) [see (Fotouhi *et al.*, 2000*b*) for details]. The vector of controls τ is represented by the torques τ_1 and τ_2, and φ is the vector of joint variables also referred to as the state variables. The states $\varphi_1, \dot{\varphi}_1$ are the rotation and angular velocity of the shoulder link, $\varphi_2, \dot{\varphi}_2$ are the rotation and angular velocity of the elbow link, and g is the gravitational acceleration. The manipulator's tip is to follow a desired trajectory given by the knots in the space (y, z). The $y - z$ coordinates of the knots can be easily converted into positions specified at the joint level (e.g. $\varphi_1 - \varphi_2$). The desired trajectory given in the joint coordinates is denoted as φ_d.

3. TRAJECTORY PLANNING

3.1 *Initial trajectory*

The geometric trajectory is obtained by N knots in the space coordinates system (y, z) given by the pairs (y_i, z_i), $i = 1, \ldots, N$. These knots can be transformed into the joint rotations φ_{1_i}, φ_{2_i} of the manipulator by the following transformation (Figure 1)

$$\varphi_1 = \alpha - \chi \tag{4}$$

$$\chi = \cos^{-1}\left(\frac{y^2 + z^2 + l_1^2 - l_2^2}{2l_1\sqrt{y^2 + z^2}}\right) \tag{5}$$

$$\alpha = \tan^{-1}\left(\frac{z}{y}\right) \tag{6}$$

$$\varphi_2 = \cos^{-1}\left(\frac{y^2 + z^2 - l_1^2 - l_2^2}{2l_1 l_2}\right) \tag{7}$$

Using these knots and considering constant time steps, dt, between the knots calculated as $dt =$

$t_f/(N-1)$ where t_f is the desired travelling time, two sets of cubic spline interpolation polynomials can be fitted to approximate the initial trajectory.

3.2 *Feasible trajectory*

The trajectory is considered feasible if the constraints imposed on the angular velocity and acceleration at each joint are met. An infeasible trajectory can be made feasible by using linear scaling to adjust the time intervals between each pair of adjacent knots.

The time variable t is replaced by the scaled time $\bar{t} = \lambda t$, where λ is the adjustment factor. The joint velocity and joint acceleration are then

$$\frac{d\varphi}{dt} = \frac{1}{\lambda}\frac{d\varphi}{dt} \qquad \frac{d^2\varphi}{d\bar{t}^2} = \frac{1}{\lambda^2}\frac{d^2\varphi}{dt^2} \tag{8}$$

The velocities and accelerations are matched for each joint to pre-specified constraints given as

$$|\dot{\varphi}_1(t)| \le VL_1 \qquad |\dot{\varphi}_2(t)| \le VL_2 \tag{9}$$

$$|\ddot{\varphi}_1(t)| \le AL_1 \qquad |\ddot{\varphi}_2(t)| \le AL_2 \tag{10}$$

The scaling factor λ can be selected as follows

$$\lambda_1 = \max(\max(\frac{|\dot{\varphi}_1(t)|}{VL_1}), \max(\frac{|\dot{\varphi}_2(t)|}{VL_2})) \tag{11}$$

$$\lambda_2 = \max(\max(\frac{|\ddot{\varphi}_1(t)|}{AL_1}), \max(\frac{|\ddot{\varphi}_2(t)|}{AL_2})) \tag{12}$$

$$\lambda = \max(1, \lambda_1, \sqrt{\lambda_2}) \tag{13}$$

Then, the scaled time variable $\bar{t}$ and the scaled velocities and accelerations are

$$\bar{t} = \lambda t \quad \dot{\varphi}(\bar{t}) = \frac{1}{\lambda}\dot{\varphi}(t) \quad \ddot{\varphi}(\bar{t}) = \frac{1}{\lambda^2}\ddot{\varphi}(t) \tag{14}$$

3.3 *Following a specified velocity profile*

In this section the fitting of a specified profile to the velocity along the trajectory is addressed. This profile of the tip of manipulator is specified as v_b^s in time. Equation (22) is an example of v_b^s.

In order to fit a feasible trajectory into this given velocity profile, a nonlinear scaling is used that adjusts individually (and differently) the time intervals between consecutive knots as follows. The time step variable dt is replaced by the scaled time step $\bar{dt} = \lambda^{(i)} dt$. The factor $\lambda^{(i)}$ is used to adjust the time step between t_i and t_{i+1} and is calculated from

$$\lambda^{(i)} = c_i\lambda_i + (1-c_i)\lambda_{i+1} \tag{15}$$

where

$$c_i = \frac{v_b^s(t_i)}{v_b^s(t_i) + v_b^s(t_{i+1})} \qquad \lambda_i = \frac{|v_b(t_i)|}{|v_b^s(t_i)|} \tag{16}$$

The velocities $v_b(t_i)$ and $v_b^s(t_i)$ are the actual and specified linear velocities of the tip of the manipulator, respectively. Next, the time variable t is replaced by the scaled time

$$\bar{t} = \bar{t}_i + \lambda^{(i)}(t - t_i) \tag{17}$$

for $t_i \le t \le t_{i+1}$ (and for $\bar{t}_i \le \bar{t} \le \bar{t}_{i+1}$). The scaled velocities and accelerations are

$$\dot{\varphi}(\bar{t}_i) = \frac{1}{\lambda^{(i)}}\dot{\varphi}(t_i) \qquad \ddot{\varphi}(\bar{t}_i) = \frac{1}{{\lambda^{(i)}}^2}\ddot{\varphi}(t_i) \tag{18}$$

The error between actual tip velocity, $v_b(\bar{t}_i)$, and specified tip velocity, $v_b^s(\bar{t}_i)$, for every scaled time step is defined as

$$E_i = E(\bar{t}_i) = \frac{|v_b(\bar{t}_i)| - |v_b^s(\bar{t}_i)|}{max(|v_b(\bar{t}_i)|, |v_b^s(\bar{t}_i)|)} \tag{19}$$

The values of E_i and the adjustment factors $\lambda^{(i)}$ in consecutive iterations indicate the convergence of the procedure. The steps above are repeated until either the least square norm $\|E\|$ is sufficiently close to zero or the norm $\|\lambda\|$ is close to one where:

$$\|E\| = \sqrt{\left(\sum_{i=1}^{N} E_i^2\right)/N} \tag{20}$$

$$\|\lambda\| = \sqrt{\left(\sum_{i=1}^{N} {\lambda^{(i)}}^2\right)/N} \tag{21}$$

The norm $\|\lambda\|$ indicates the rate of scaling at the knots for each iteration. There is no further improvement when this norm reaches one. Some limits on $\lambda^{(i)}$ can be imposed to obtain a smooth convergence of the iterations, such as, $\lambda_{min} \le \lambda^{(i)} \le \lambda_{max}$, where $\lambda_{min} < 1$, and $\lambda_{max} > 1$. For simulation purposes the following limits were used: $\lambda_{min} = 0.5$, $\lambda_{max} = 1.5$ for the first iteration; and $\lambda_{min} = 0.25$, $\lambda_{max} = 4.0$ for other iterations.

4. SIMULATION RESULTS

For simulation purposes a trajectory of the shape shown in Figure 2, consisting of two linear pieces, with a particular tip velocity profile and obeying angular velocity and acceleration constraints, was considered. The initial and the desired trajectories in the horizontal $y-z$ plane ($g = 0$) are shown in this figure. As shown in Figure 1, I_1 and I_2 are the mass moment of inertia of the links w.r.t. their centers of mass, m_1 and m_2 are the masses of the shoulder and the elbow links, respectively, m_a is the

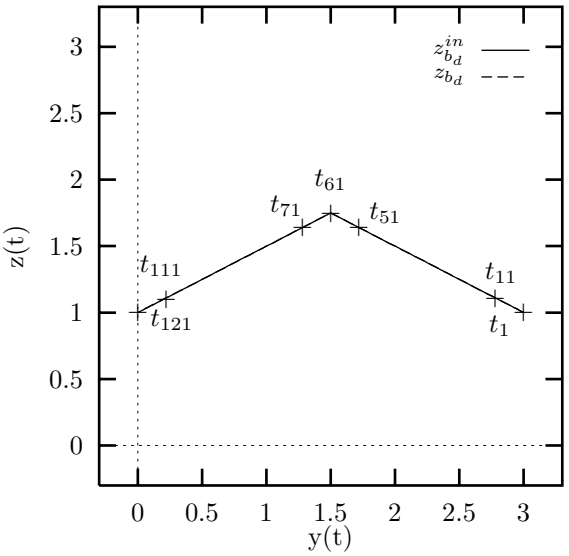

Fig. 2. Initial, $z^{in}_{b_d}$, and desired, z_{b_d}, trajectories, which practically coincided.

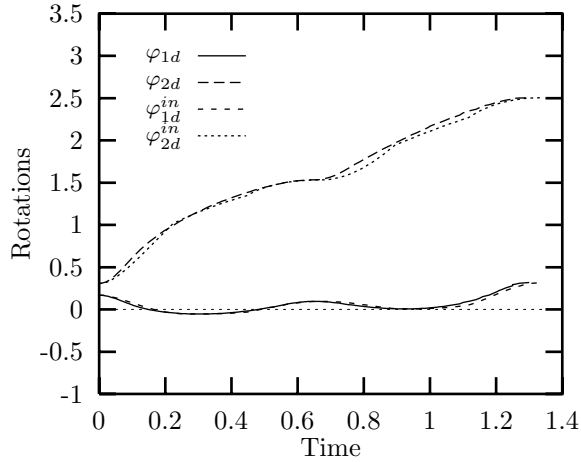

Fig. 3. Rotations of the links for the desired and initial paths.

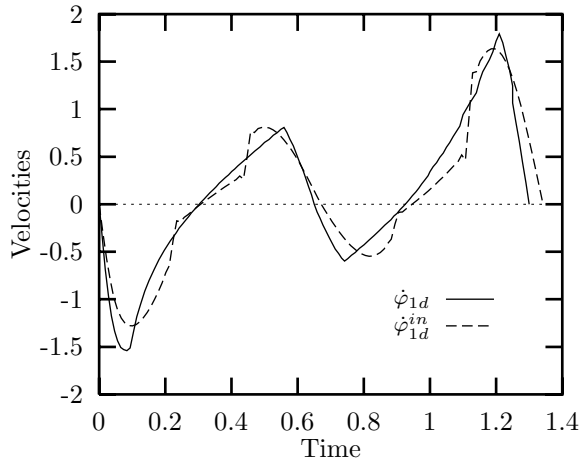

Fig. 4. Angular velocity of the shoulder link for the desired, $\dot{\varphi}_{1d}$, and initial, $\dot{\varphi}^{in}_{1d}$, paths.

mass at the elbow joint, and m_b is the mass at the tip of the manipulator. This mass differs between the stops. The lengths of the links are l_1 and l_2, whereas l_{c1}, l_{c2} locate the centers of mass of the links. In the simulation the physical parameters of the manipulator were set as those given in Figure 1.

For the cubic spline interpolation 121 knots (points position) were chosen along the curve. For the case presented here, the desired profile of linear tip velocity, v^s_b, was specified as

$$\begin{aligned}
v^s_b &= 3.0\frac{t-t_1}{t_{11}-t_1} && \text{for } t_1 \le t \le t_{11}\\
v^s_b &= 3.0 && \text{for } t_{11} \le t \le t_{51}\\
v^s_b &= 3.0\frac{(t_{61}-t)}{t_{61}-t_{51}} && \text{for } t_{51} \le t \le t_{61}\\
v^s_b &= 3.0\frac{(t-t_{61})}{t_{71}-t_{61}} && \text{for } t_{61} \le t \le t_{71}\\
v^s_b &= 3.0 && \text{for } t_{71} \le t \le t_{111}\\
v^s_b &= 3.0\frac{t_{121}-t}{t_{121}-t_{111}} && \text{for } t_{111} \le t \le t_{121}
\end{aligned} \tag{22}$$

where $t^{in}_1 = 0$, $t^{in}_{11} = \frac{t^{in}_f}{12}$, $t^{in}_{51} = \frac{5t^{in}_f}{12}$, $t^{in}_{61} = \frac{t^{in}_f}{2}$, $t^{in}_{71} = \frac{7t^{in}_f}{12}$, $t^{in}_{111} = \frac{11t^{in}_f}{12}$, and $t^{in}_{121} = t^{in}_f = 1.34$ are also indicated in Figure 2. The final time t^{in}_f (seconds) was calculated using $s = \int_0^{t^{in}_f} v^s_b dt$ where $s = 3.354\ m$ is the known distance travelled by the manipulator tip and v^s_b is specified by Equation (22). The cubic spline interpolation of the angles of rotation versus time for the initial ($\varphi^{in}_{1_d}$, $\varphi^{in}_{2_d}$) and desired (φ_{1_d}, φ_{2_d}) maneuvers are plotted in Figure 3. The angular velocity of the shoulder ($\dot{\varphi}^{in}_{1d}$, $\dot{\varphi}_{1d}$) and elbow links ($\dot{\varphi}^{in}_{2d}$, $\dot{\varphi}_{2d}$), and the linear tip velocity of the manipulator (v^{in}_b, v^s_b, v_b), are shown in Figures 4, 5 and 6 respectively.

For the first and last knots in the cubic spline interpolation the following conditions were used: $\dot{\varphi}_{1_1} = \dot{\varphi}_1(0) = 0$, $\dot{\varphi}_{1_N} = \dot{\varphi}_1(t_f) = 0$, $\dot{\varphi}_{2_1} = \dot{\varphi}_2(0) = 0$, and $\dot{\varphi}_{2_N} = \dot{\varphi}_2(t_f) = 0$. The velocity ($VL_1, VL_2$) and acceleration ($AL_1, AL_2$) constraints for each joint were $VL_1 = 5$ [rad/s], $VL_2 = 5$ [rad/s], $AL_1 = 100$ [rad/s^2], $AL_2 = 100$ [rad/s^2]. As can be observed from Figures 4 and 5 for the initial trajectory, the angular velocity of the shoulder and elbow links reached about 1.5 rad/s and 4 rad/s respectively. The angular acceleration of the shoulder and elbow links reached 100 rad/s^2 and -300 rad/s^2 respectively, which clearly violated the constraints imposed on the angular acceleration of the joints. The procedure discussed in section 3.2 (using the linear scaling of time) was applied to satisfy the constraints on the angular velocity and acceleration of the joints.

The trajectory was next modified using the new nonlinear scaling of the time described in section 3.3 so as to approach the desired profile of the tip velocity, which resulted in a maneuver time of $t_f =$

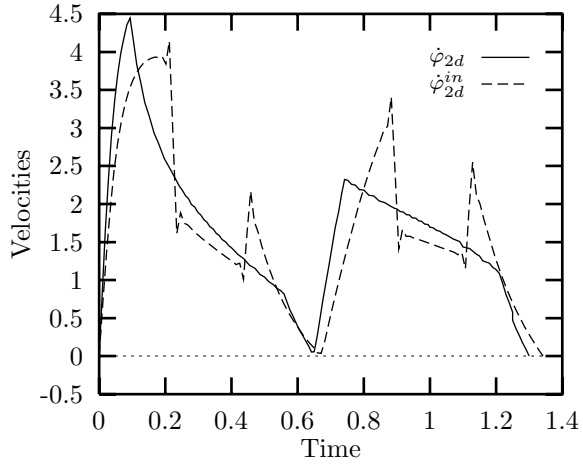

Fig. 5. Angular velocity of the elbow link for the desired, $\dot{\varphi}_{2d}$, and initial, $\dot{\varphi}^{in}_{2d}$, paths.

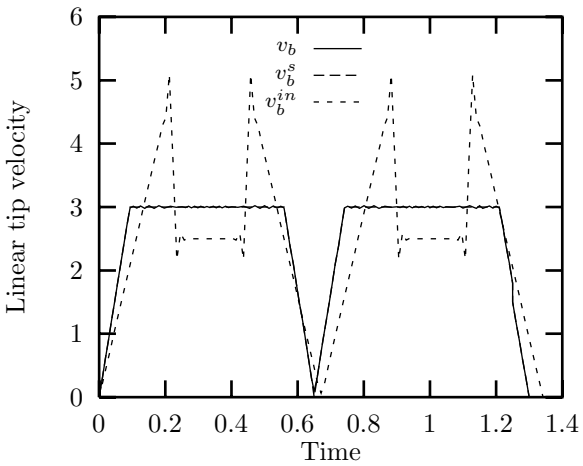

Fig. 6. Linear velocities of tip of the manipulator for the desired, v_b, specified, v^s_b, and initial, v^{in}_b, paths.

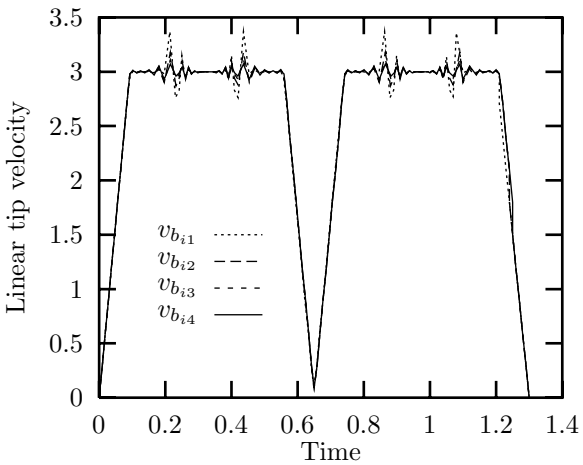

Fig. 7. Linear velocity of tip of the manipulator for the desired path, v_b, in different iterations.

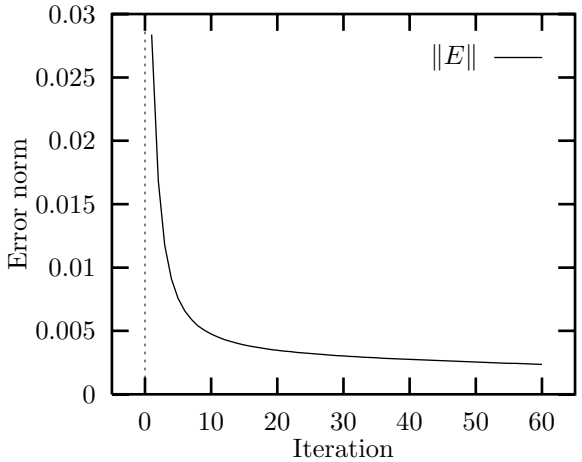

Fig. 8. Error norm $\|E\|$ as a function of iteration for $N = 121$.

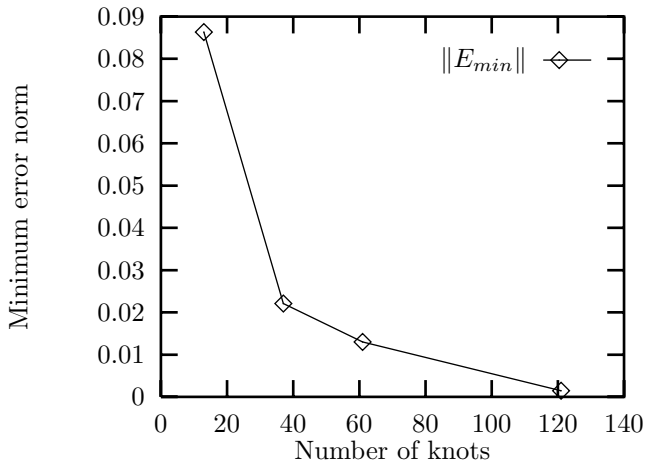

Fig. 9. Minimum of error norm $\|E\|$ as a function of number of knots.

1.3 seconds as shown in Figure 6. Figure 7 shows the convergence of the procedure for fitting this linear velocity, v_b, to its specified profile, v^s_b. As can be seen from this figure, v_b almost converges to v^s_b after only four iterations which can be attributed to the limiting value of λ_{min} and λ_{max}. Figures 8 and 10 show the first error norm and second error norm for the convergence of iteration for speed planning. As can be seen from Figure 8, for $N = 121$ the error norm could not be reduced to less than about .0025, which can be attributed to the number of knots chosen. Actually, when the error norm reached a small value, in this case .004, the second error norm reached one in only ten iterations. It was found that the greater the number of knots the smaller the error. For example, as shown in Figure 9, doubling the number of knots to $N = 121$, decreased the error approximately six times to .0025. The second norm or λ-norm, shown in Figure 10 for $N = 121$, was used to determine the best solution (iteration) when the first error norm could not be reduced any further. The set that caused the least fluctuations of $\lambda^{(i)}$ was selected, that is the set for which $|(1-\|\lambda\|)|$ is minimum.

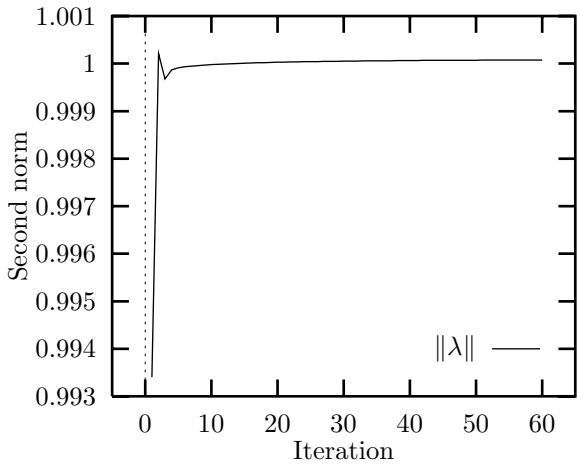

Fig. 10. Second norm $\|\lambda\|$ as a function of iteration for $N = 121$.

5. CONCLUSIONS

A two-phase trajectory planning for a two-link rigid manipulator was presented. The problem was solved in two stages. First, a geometric trajectory planning using cubic spline functions was performed to construct an initial trajectory. The motion constraints (maximum angular velocity and maximum angular acceleration) were met using a linear scaling of the time variable. Then a new approach was applied to the speed control (fitting the manipulator's tip velocity to a pre-specified profile) using a nonlinear scaling of the time variable. It was demonstrated that the specified velocity profile can be followed very closely. The method used here can be implemented to follow any specified speed profile very closely. Simulation results were presented which show the convergence and effectiveness of the path planning approach.

6. REFERENCES

Craig, John J. (1986). *Introduction to Robotics*. Addison-Wesley. Reading, Massachusetts.

Fotouhi, Reza, Walerian Szyszkowski and Peter Nikiforuk (2000*a*). Trajectory planning and speed control for a two-link rigid manipulator. *Journal of Mechanical Design, Transactions of the ASME*. Accepted for publication.

Fotouhi, Reza, Walerian Szyszkowski, Peter N. Nikiforuk and Madan M. Gupta (2000*b*). Parameter identification and trajectory following of a two-link rigid manipulator. *Journal of Systems and Control Engineering, Proceedings Institution of Mechanical Engineers, Part I* **213**, 455–466.

Schumaker, Larry L. (1981). *Spline functions : basic theory*. John Wiley & Sons Ltd. New York ; Toronto.

Simon, Dan and Can Isik (1991). Optimal trigonometric robot joint trajectories. *Robotica* **9**, 379–386.

Srinivasan, L. N. and Q. Jeffrey Ge (1998). Fine tuning of rational b-spline motions. *Journal of Mechanical Design, Transactions of the ASME* **120**, 46–51.

Thompson, Stuart E. and Rajnikant V. Patel (1987). Formulation of joint trajectories for industrial robot using b-splines. *IEEE Transactions on Industrial Electronics* **34**(2), 192–199.

Wang, Chi-Hsu and Jong-Gin Horng (1990). Constrained minimum-time path planning for robot manipulators via virtual knots of the cubic b-spline functions. *IEEE Transactions on Automatic Control* **35**(5), 573–577.

Wu, Chi-haur and Chi-cheng Jou (1991). Design of a controlled spatial curve trajectory for robot manipulations. *ASME Journal of Dynamic Systems, Measurement, and Control* **113**, 248–258.

Xiangrong, Xu and Ma Xiangfeng (1994). A method for trajectory planning of robot manipulators. *Modelling, Measurement & Control, B, ASME Press* **54**(3), 33–36.